

Oxygen priming induced by elevated CO₂ reduces carbon accumulation and methane emissions in coastal wetlands

Received: 8 April 2022

Accepted: 10 October 2022

Published online: 05 January 2023

 Check for updates

Genevieve L. Noyce¹✉, **Alexander J. Smith**², **Matthew L. Kirwan**²,
Roy L. Rich¹ & **J. Patrick Megonigal**¹✉

Warming temperatures and elevated CO₂ are inextricably linked global change phenomena, but they are rarely manipulated together in field experiments. As a result, ecosystem-level responses to these interacting facets of global change remain poorly understood. Here we report on a four-year field manipulation of warming and elevated CO₂ in a coastal wetland. Contrary to our expectations, elevated CO₂ combined with warming reduced the rate of carbon accumulation due to increases in plant-mediated oxygen flux that stimulated aerobic decomposition via oxygen priming. Evidence supporting this interpretation includes an increase in soil redox potential and a decrease in the nominal oxidation state of the dissolved organic carbon pool. While warming alone stimulated methane (CH₄) emissions, we found that elevated CO₂ combined with warming reduced net CH₄ flux due to plant–microbe feedbacks. Together, these results demonstrate that ecosystem responses to interacting facets of global change are mediated by plant traits that regulate the redox state of the soil environment. Thus, plant responses are critical for predicting future ecosystem survival and climate feedbacks.

The redox state of soils is a fundamental control on greenhouse gas fluxes and ecosystem-level responses to global change drivers such as elevated CO₂ (eCO₂) and warming. Interactions between plants and microbes drive redox-active biogeochemical processes that remain poorly understood and yet dictate ecosystem feedbacks on climate and long-term ecosystem resilience¹. Plants alter the biogeochemistry of the local soil environment by regulating the soil redox environment as sources of both electron donors (carbon) and electron acceptors (oxygen)². Deposition of organic carbon sequesters CO₂ from the atmosphere, but these easily degradable carbon compounds also stimulate heterotrophic microbial respiration³. In uplands, plants stimulate oxygen consumption in the rhizosphere through root exudation and root turnover, creating hypoxic and anoxic microsites that facilitate carbon preservation^{4,5}. Vascular plants adapted to wetlands and other saturated systems stimulate oxygen consumption

through root exudates but also enhance oxygen supply through plant oxygen transport, potentially stimulating aerobic decomposition and other aerobic microbial processes such as methanotrophy^{6,7}. This oxygen is rapidly consumed⁸ through abiotic and biotic oxidation reactions that raise soil redox potential and regenerate alternative electron acceptors⁴.

Although eCO₂ often stimulates plant productivity, carbon sequestration and carbon-limited microbial processes such as methanogenesis^{9–12}, feedbacks arising from plant–microbe interactions can cause the opposite responses^{13–16}. In particular, aerobic biogeochemical processes are largely overlooked in wetland ecosystems but could, in theory, reduce carbon sequestration and methane (CH₄) emissions in response to interacting global change factors such as eCO₂ and warming. This interdependence of plant and microbial metabolism means that ecosystem responses to climate change can

¹Smithsonian Environmental Research Center, Edgewater, MD, USA. ²Virginia Institute of Marine Science, College of William and Mary, Gloucester Point, VA, USA. ✉e-mail: noyceg@si.edu; megonigalp@si.edu

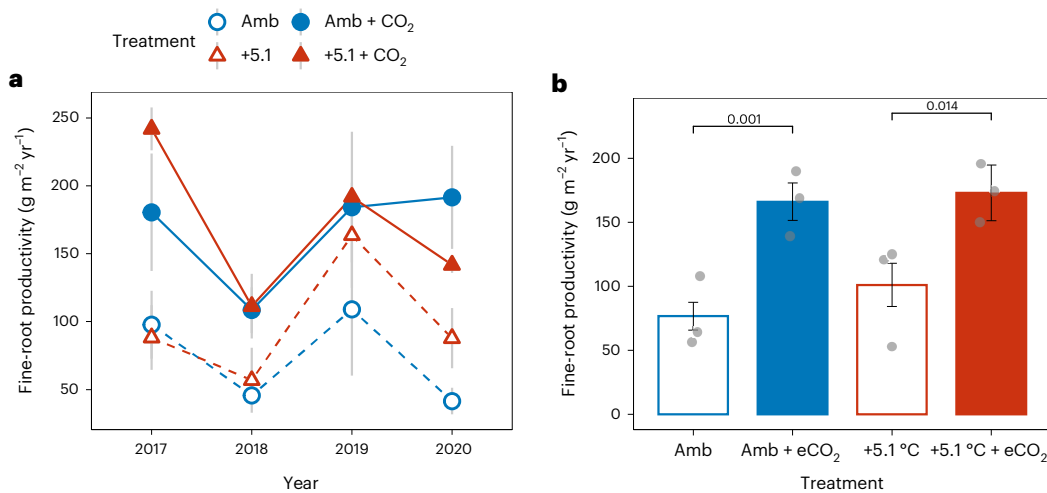


Fig. 1 | Fine-root productivity in ambient and warmed plots with and without elevated CO₂. **a**, Fine-root productivity for individual years. Points are means of triplicate plots. **b**, Fine-root productivity averaged across all four years. Bars are means of triplicate plots. Brackets above the paired bars show the *P* values for the

differences between treatments based on Tukey's honestly significant difference test. eCO₂ significantly increased mean root productivity in both ambient (blue) and warmed (red) treatments. Error bars are s.e. across treatment replicates (*n* = 3).

be thoroughly understood only through manipulations that include both above-ground and below-ground components. We actively manipulated whole-ecosystem temperature and CO₂ concentration in a tidal marsh on the Chesapeake Bay to investigate redox-mediated biogeochemical responses. We hypothesized that soil carbon sequestration and CH₄ emissions would increase in response to both warming and eCO₂ as individual perturbations^{9–12} and that the interaction of these drivers would be multiplicative due to the combination of increased plant carbon inputs and temperature stimulation of methanogenic activity. However, we show here that redox shifts induced by eCO₂ instead led to simultaneous reductions in carbon accumulation and CH₄ emissions, which we propose were caused by oxygen priming¹⁷.

Effects on plant biomass and soil redox potential

Plants allocate biomass between roots and shoots to optimize uptake of CO₂ (above-ground biomass) versus water and nutrients (below-ground biomass). In saturated systems, root–shoot allocation and productivity may have strong redox feedbacks that determine the carbon sequestration capacity of the ecosystem¹⁸. Previously, we reported that eCO₂ significantly increased root productivity relative to ambient conditions in the initial two years of a warming × eCO₂ experiment¹⁹. This trend continued through the next two years (Fig. 1A), with eCO₂ increasing mean fine-root productivity by an average of 116% under ambient-temperature conditions (*P* < 0.001) and 71% under warmed conditions (*P* = 0.014) over the four years (Fig. 1B). There was no significant effect of warming by 5.1 °C on root productivity under either ambient (*P* = 0.719) or elevated (*P* = 0.991) CO₂ conditions. Warming also did not affect the stem density of *Schoenoplectus americanus* (*P* = 0.158), but eCO₂ significantly increased stem density (*P* = 0.001) (Extended Data Fig. 1).

We propose that the high stem density and high root productivity in the eCO₂ plots led to an increase in plant-mediated oxygen transport into the soil, driving changes in microbial respiration pathways and overall ecosystem functioning. To test this theory of oxygen priming, we developed an automated approach for tracking soil redox potential and used it to measure redox every 30 min starting in April 2020 (Fig. 2). These high-frequency data illustrated that redox potential was significantly higher under warming and eCO₂ compared with warming alone (*P* < 0.001). This consistent oxidizing effect of eCO₂ was especially pronounced in the shallow rooting zone (5 cm) and was observed under ambient temperatures (Extended Data Fig. 2). By contrast, eCO₂ had

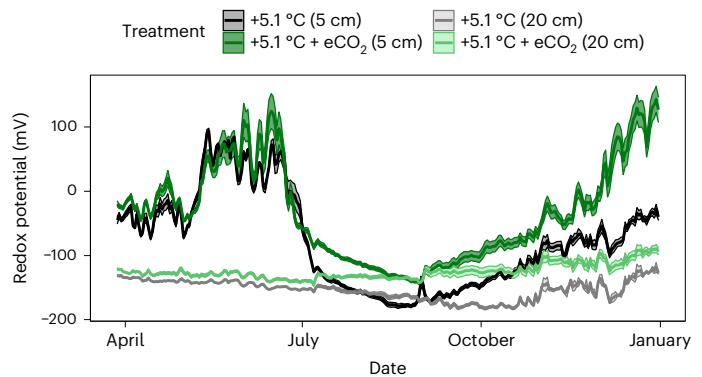


Fig. 2 | Automated redox data in warmed plots with and without elevated CO₂ from April 2020 to December 2020. Lines show daily average, and error bands are ±2 s.e. (*n* = 3); colours indicate depth and treatment. Redox potential is measured in each plot every 30 min. Data have been adjusted to be in reference to the standard hydrogen electrode.

only subtle effects on SO₄ concentration and pH (Supplementary Figs. 2 and 3). Due to the high-organic, low-metal content of these soils, oxygen, SO₄ and pH are the only substrates likely to explain the eCO₂ effects on redox. As SO₄ and pH cannot explain the strong variability we see in the redox data, we propose that this indicates a shift in microbial respiration towards oxygen-dependent processes stimulated by root oxygen loss²⁰. The amount of oxygen transported by plants and released through root oxygen loss has been previously presumed to be related to a variety of factors²¹ such as diffusive versus mass flow mechanisms²⁰, stem density²², root length and diameter²³, root suberin content and aerenchyma tissue, all of which vary strongly across plant species. Our results suggest the need to also assess whether exposure to eCO₂ fundamentally changes these characteristics and the mechanisms by which plants transport oxygen into soils.

Soil redox reflects thermodynamic constraints on the structure of carbon compounds that can be degraded when coupled to various electron acceptors²⁴. Although carbon compounds are commonly classified as ‘recalcitrant’ or ‘labile’, all carbon compounds can ultimately be degraded by microbial communities, just at different rates²⁵. Calculating the nominal oxidation state of carbon (NOSC) creates

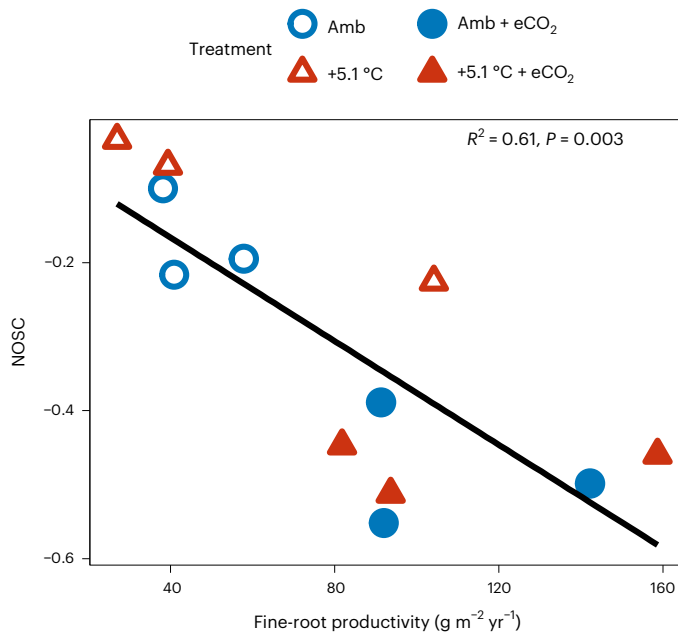


Fig. 3 | Root productivity versus mean NOSC for porewater DOC. Statistics show results of linear regression. Fine roots were retrieved from root ingrowth cores deployed November 2017–November 2018. Porewater was collected from 20 cm depth in July 2018 and analysed using Fourier-transform ion cyclotron resonance mass spectrometry.

a thermodynamically relevant metric for assessing organic-matter quality²⁶. In low-redox environments characteristic of saturated soils, the bioavailability of soil carbon compounds is determined both by NOSC and by the specific terminal electron acceptor to which it is coupled^{4,27}. Compounds that are not thermodynamically favourable to degrade in the absence of oxygen will be preserved under anaerobic conditions^{4,5,26}.

To determine the effect of eCO₂ on NOSC in a field setting, we measured the NOSC of shallow (20 cm depth) porewater dissolved organic carbon (DOC) from each treatment and found that although there was no effect of warming on porewater NOSC ($P = 0.773$), eCO₂ reduced NOSC from an average (\pm standard error (s.e.)) of -0.14 ± 0.03 to -0.48 ± 0.02 ($P < 0.001$). NOSC was also strongly negatively correlated with root productivity (Fig. 3). As with the redox data, we propose that the NOSC of porewater DOC declined because exposure to eCO₂ stimulated root oxygen loss, increasing the supply of a thermodynamically favourable terminal electron acceptor (oxygen) and thereby stimulating microbial oxidation of previously preserved DOC compounds. Solid-phase organic carbon is probably also degraded at higher rates under these conditions, which would lead to loss of previously preserved soil organic matter²⁶.

Implications for wetland persistence

The resilience of tidal wetlands to sea-level rise depends on their ability to build elevation at a rate comparable to the rate of sea-level rise²⁸. Tidal wetlands with low rates of mineral sediment deposition, such as the present site, accrete almost entirely through autotrophic sub-surface expansion driven by the balance between root production and decomposition and are considered the most vulnerable to sea-level rise^{18,28,29}. Previously, we have shown that soil accretion rates closely track below-ground productivity²⁹. As a result, global change drivers that increase below-ground production (such as eCO₂ in this experiment) are expected to stimulate soil surface accretion^{9,30}; however, this assumption does not account for redox shifts or oxygen priming driving an increase in rates of aerobic decomposition.

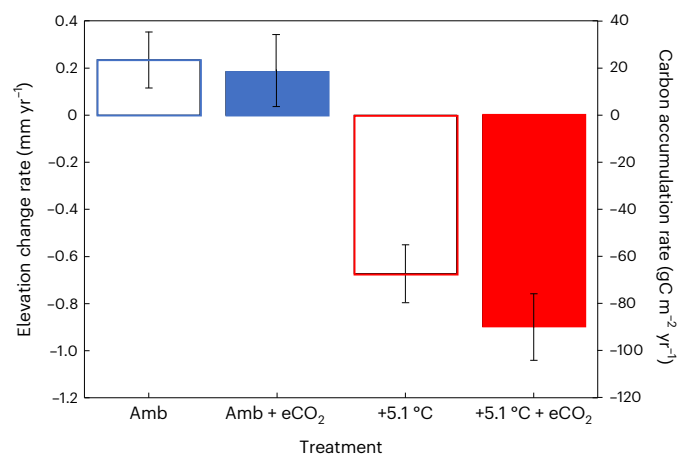


Fig. 4 | Average rate of change in marsh surface elevation and carbon accumulation from January 2017 to August 2020. Carbon accumulation was calculated as the product of elevation change ($n = -160$) in each experimental plot and the average carbon density at the site (104.8 kgC m^{-3}). Error bars are s.e. across treatment replicates ($n = 3$).

In contrast to our hypothesis, we found that neither warming nor eCO₂ increased soil elevation relative to ambient conditions (Fig. 4) despite the large increases in root productivity observed under eCO₂ (Fig. 1b). This contrasts with previous work from other experiments at this site, which consistently found that eCO₂ enhanced soil elevation gain^{9,31}. Wetland plants add both carbon and oxygen to the soil in amounts that scale with biomass production; contrary to our expectation, under eCO₂, the balance of these processes favours relatively higher rates of aerobic decomposition and a consequent decline in soil surface accretion. Therefore, previous estimates that integrate feedbacks between atmospheric CO₂ and carbon sequestration on the basis of ephemeral plant biomass responses may not apply to soil carbon stocks, which are considerably more important for the long-term carbon storage capacity of ecosystems. In addition, the lack of elevation (and thus carbon sequestration) response indicates that, despite increased root productivity, these ecosystems remain vulnerable to sea-level rise under current temperature conditions and projected future warming will exacerbate this vulnerability. Our results indicate that elevated root production under future climate conditions may not always increase marsh resilience as previously assumed due to antagonistic feedbacks between increased root production and aerobic decomposition.

Effects on methane emissions

Decomposition in anaerobic environments proceeds through multiple interacting microbial processes that influence carbon storage and emissions of greenhouse gases, including CH₄. Warming substantially increased CH₄ production and emissions, in all years of the experiment (Fig. 5a), probably due to cascading effects of increased soil temperature on plant carbon inputs and rates of microbial metabolism³². Throughout the duration of the experiment, there was a 317% increase in summer CH₄ emissions with +5.1 °C of warming compared with ambient plots ($P < 0.001$; Fig. 5b). This mirrors a 141% increase in porewater CH₄ in the warmed plots ($P < 0.001$; Extended Data Fig. 3). The expectation that warming stimulates wetland CH₄ emissions is supported by a previous report from the present warming study³² and numerous other studies that manipulated temperature without also manipulating atmospheric CO₂^{33–35}, two factors that are inextricably linked.

Contrary to our hypothesis, eCO₂ substantially dampened warming-induced increases in CH₄ emissions. Methane emissions

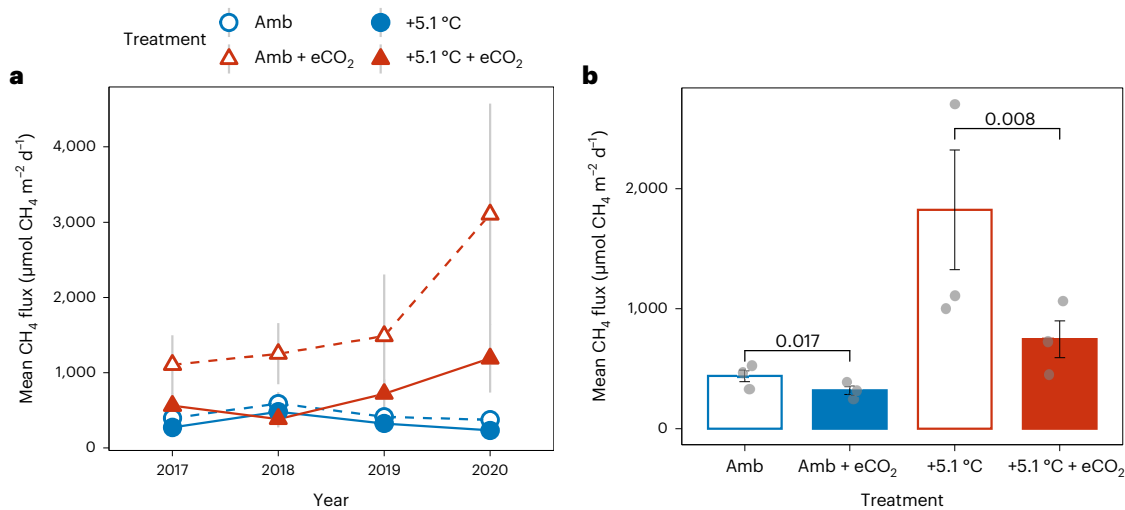


Fig. 5 | Summer CH₄ emissions in ambient and warmed plots with and without elevated CO₂. a, Summer (June–August) CH₄ emissions for individual years. Points are means of triplicate plots. **b**, Mean summer CH₄ emissions averaged across all four years. Bars are means of triplicate plots. Brackets above the paired

bars show the *P* values for the differences between treatments based on Tukey's honestly significant difference test. Elevated CO₂ significantly reduced mean CH₄ emissions in both ambient and warmed treatments. Error bars are s.e. across treatment replicates (*n* = 3).

from warmed plots also exposed to eCO₂ were not significantly higher than emissions from ambient-temperature plots across the four years (*P* = 0.171; Fig. 5b). Elevated CO₂ also significantly reduced summer CH₄ emissions within each of the two warming treatments. At ambient temperatures, eCO₂ reduced mean CH₄ emissions by 27% (*P* = 0.017) and porewater CH₄ by 54% (*P* = 0.004) (Fig. 5b and Extended Data Fig. 3). The negative effect of eCO₂ on CH₄ emissions was even stronger in the +5.1 °C treatment, where eCO₂ reduced mean emissions by 59% (*P* = 0.008) and porewater CH₄ by 15% (*P* = 0.031) (Fig. 5b and Extended Data Fig. 3).

Our results contrast with previous eCO₂ experiments in a variety of ecosystems where eCO₂ stimulated CH₄ emissions^{10,36–40}, typically driven by an increase in labile carbon supplied to the methanogenic community through root exudation or turnover^{40,41}. However, plants are sources of both carbon (required for CH₄ production) and oxygen (required for aerobic CH₄ oxidation), meaning that global change factors can either increase or decrease CH₄ emissions depending on the net balance of these processes¹³. While warming stimulated CH₄ production more than CH₄ oxidation³², we propose that eCO₂ stimulated CH₄ oxidation more than CH₄ production. Species-specific plant traits can lead to opposing effects on net CH₄ emissions^{12,13,42,43}. We propose that *S. americanus* creates a net oxidizing effect on the rhizosphere³², especially under warming and eCO₂ (Fig. 2), such that the root oxygen loss effect outperforms the carbon exudate effect, reducing net CH₄ emissions. Although the capacity of *S. americanus* to oxidize the rhizosphere has not been determined, the species is morphologically similar to *Scirpus lacustris*, which is known to transport substantial oxygen into the rhizosphere, especially during the growing season⁴⁴. In addition, mesocosm experiments have found that soil redox potential increases with *S. americanus* root biomass, suggesting that more root productivity leads to increasingly oxidized soil environments¹⁷. A similar net oxidizing effect has also been observed in non-tidal wetlands dominated by *Carex lasiocarpa*, where an eCO₂-driven reduction in net CH₄ emissions was associated with increases in soil redox potential, similar to what we found here, and an increase in methanotroph abundance¹³. It is likely that this oxidation effect scales across a range of stem densities, (as we have previously shown that CH₄ emissions decline with increasing *S. americanus* biomass⁴²) and persists beyond the growing season as senescent stems continue to transport oxygen into saturated soils⁴⁵.

Our results also contrast with previous work in *S. americanus*-dominated areas of this site, all of which found that eCO₂ enhanced, rather than suppressed, CH₄ emissions^{38,42,46}. The most likely explanation for this difference is that the current study has reached a higher density of *S. americanus* stems than previous experiments. Although *S. americanus* stimulates CH₄ oxidation across a broad range of stem densities⁴², it simultaneously stimulates CH₄ production by adding labile carbon to the system through root exudates and root turnover. Thus, the net effects of eCO₂ on CH₄ emissions can theoretically range from a reduction in the size of the positive response to a negative response (net decrease) as observed in the present experiment. A separate experiment that began in 1987³⁸ found that eCO₂ increased CH₄ emissions, but those plots had an average *S. americanus* density of 364 stems m⁻², 30% less than the lowest sedge biomass in our current experiment (Extended Data Fig. 1). Overall, the present and previous work at this site suggests that ecosystem responses to eCO₂ vary with individual plant traits and ecosystem-scale variables such as stem density. Importantly, these redox-mediated effects influence both soil carbon sequestration and CH₄ emissions. Because eCO₂ effects on *S. americanus* stem density and root biomass can persist over decades^{47,48}, our observed suppression of soil carbon sequestration and CH₄ emissions is probably a long-term response that will continue unless other factors intervene to suppress the initial eCO₂ response.

Implications for radiative forcing

The net effect of global change drivers on greenhouse gas emissions has consequences for ecosystem–climate feedbacks and the long-term efficacy of management practices designed to mitigate greenhouse gas emissions⁴⁹. In this experiment, the net effect of warming on carbon sequestration (Fig. 4) and CH₄ emissions (Fig. 5) was an increase in radiative forcing compared with ambient treatments (Fig. 6). Notably, the significant reduction in CH₄ emissions driven by eCO₂ (Fig. 5) did not significantly mitigate the increase in radiative forcing attributed to lower soil carbon sequestration rates under eCO₂ compared with the warming alone (*P* = 0.582; Fig. 6), as quantified by the loss of elevation (Fig. 4).

Warming temperatures and eCO₂ are inextricably linked global change phenomena, yet they are rarely manipulated together in field experiments. Previous work has found that warming and eCO₂ can separately increase rates of wetland soil development^{48,49,50,51}. However,

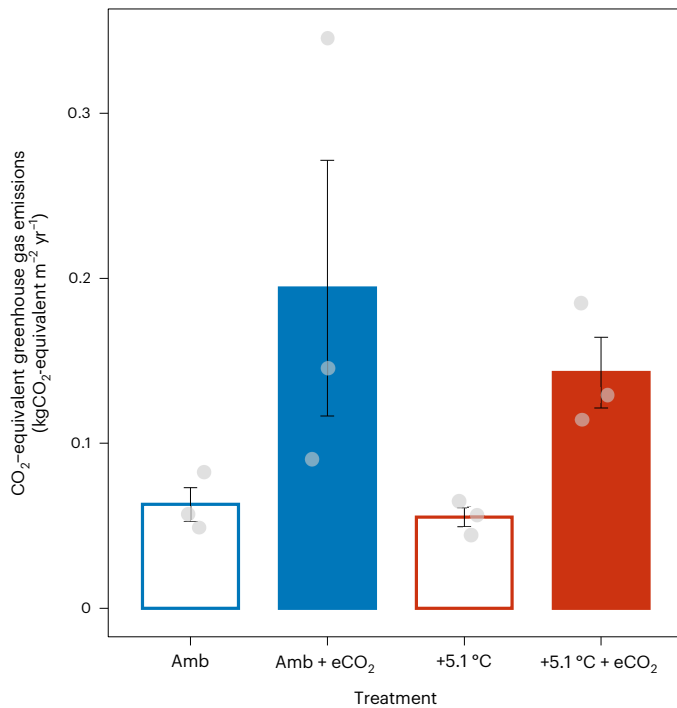


Fig. 6 | CO₂-equivalent greenhouse gas emissions by treatment averaged across the four years of the fully crossed experiment. Bars are means of triplicate plots. Error bars are s.e. across treatment replicates ($n = 3$). The equivalency of CO₂ and CH₄ radiative forcing is based on a sustained-flux global warming potential for CH₄ of 45.

our results indicate that eCO₂-driven increases in root productivity, which should make the system more reducing and preserve organic carbon, can instead make the system more oxidizing to such an extent that it quantitatively alters whole-ecosystem carbon sequestration and exacerbates tidal marsh vulnerability to sea-level rise, especially when crossed with warming. The degree to which these responses can be generalized to other ecosystems depends on the traits of the dominant plant species and the extent to which the traits are expressed in a given ecosystem and suite of environmental conditions.

Trait-based plant ecology has recently been recognized as a key discipline required to effectively model terrestrial ecosystem structure and function^{51–53}. We propose that further research on redox-relevant plant traits will make it possible to forecast the conditions under which ecosystems will become more reducing or oxidizing in response to global change, providing information required for predictive models and management policies in our changing climate⁵⁴. At present, we understand much about the anatomical, morphological and physiological mechanisms by which wetland plants transport oxygen to soils^{20,21,55} but very little about how redox-relevant traits are expressed in situ or how they vary across plant species, environmental settings, competitive interactions, disturbances or global change forcing. We know even less about how trait variation translates quantitatively into soil redox state. Our finding that trait-based plant dynamics play a key role in regulating the redox state of the soil environment suggests that our ability to forecast ecosystem resilience to global change is presently limited by a lack of methods for relating plant traits to soil redox potential in field settings.

Online content

Any methods, additional references, Nature Research reporting summaries, source data, extended data, supplementary information, acknowledgements, peer review information; details of

author contributions and competing interests; and statements of data and code availability are available at <https://doi.org/10.1038/s41561-022-01070-6>.

References

1. Heimann, M. & Reichstein, M. Terrestrial ecosystem carbon dynamics and climate feedbacks. *Nature* **451**, 289–292 (2008).
2. Wardle, D. A. et al. Ecological linkages between aboveground and belowground biota. *Science* **304**, 1629–1633 (2004).
3. Girkin, N. T., Turner, B. L., Ostle, N., Craigan, J. & Sjögersten, S. Root exudate analogues accelerate CO₂ and CH₄ production in tropical peat. *Soil Biol. Biochem.* **117**, 48–55 (2018).
4. Keiluweit, M., Nico, P. S., Kleber, M. & Fendorf, S. Are oxygen limitations under recognized regulators of organic carbon turnover in upland soils? *Biogeochemistry* **127**, 157–171 (2016).
5. Keiluweit, M., Wanzek, T., Kleber, M., Nico, P. & Fendorf, S. Anaerobic microsites have an unaccounted role in soil carbon stabilization. *Nat. Commun.* **8**, 1771 (2017).
6. Fritz, C. et al. Zero methane emission bogs: extreme rhizosphere oxygenation by cushion plants in Patagonia. *New Phytol.* **190**, 398–408 (2011).
7. Philippot, L., Hallin, S., Börjesson, G. & Baggs, E. M. Biochemical cycling in the rhizosphere having an impact on global change. *Plant Soil* **321**, 61–81 (2009).
8. Waldo, N. B., Hunt, B. K., Fadely, E. C., Moran, J. J. & Neumann, R. B. Plant root exudates increase methane emissions through direct and indirect pathways. *Biogeochemistry* **145**, 213–234 (2019).
9. Langley, J. A., McKee, K. L., Cahoon, D. R., Cherry, J. A. & Megonigal, J. P. Elevated CO₂ stimulates marsh elevation gain, counterbalancing sea-level rise. *Proc. Natl Acad. Sci. USA* **106**, 6182–6186 (2009).
10. Megonigal, J. P. & Schlesinger, W. H. Enhanced CH₄ emissions from a wetland soil exposed to elevated CO₂. *Biogeochemistry* **37**, 77–88 (1997).
11. Langley, J. A., Mozdzer, T. J., Shepard, K. A., Hagerty, S. B., & Megonigal, J. P. Tidal marsh plant responses to elevated CO₂, nitrogen fertilization, and sea level rise. *Glob. Change Biol.* **19**, 1495–1503 (2013).
12. Bridgman, M. J., Lomax, B. H. & Sjögersten, S. Impacts of elevated atmospheric CO₂ and plant species composition on methane emissions from subarctic wetlands. *Wetlands* **40**, 609–618 (2020).
13. Lin, Y. et al. Divergent responses of wetland methane emissions to elevated atmospheric CO₂ dependent on water table. *Water Res.* **205**, 117682 (2021).
14. Carney, K. M., Hungate, B. A., Drake, B. G. & Megonigal, J. P. Altered soil microbial community at elevated CO₂ leads to loss of soil carbon. *Proc. Natl Acad. Sci. USA* **104**, 4990–4995 (2007).
15. van Groenigen, K. J., Osenberg, C. W. & Hungate, B. A. Increased soil emissions of potent greenhouse gases under increased atmospheric CO₂. *Nature* **475**, 214–216 (2011).
16. van Groenigen, K. J. et al. Faster turnover of new soil carbon inputs under increased atmospheric CO₂. *Glob. Change Biol.* **23**, 4420–4429 (2017).
17. Wolf, A. A., Drake, B. G., Erickson, J. E. & Megonigal, J. P. An oxygen-mediated positive feedback between elevated carbon dioxide and soil organic matter decomposition in a simulated anaerobic wetland. *Glob. Change Biol.* **13**, 2036–2044 (2007).
18. Rietl, A. J., Megonigal, J. P., Herbert, E. R. & Kirwan, M. L. Vegetation type and decomposition priming mediate brackish marsh carbon accumulation under interacting facets of global change. *Geophys. Res. Lett.* **48**, e2020GL092051 (2021).
19. Noyce, G. L., Kirwan, M. L., Rich, R. L. & Megonigal, J. P. Asynchronous nitrogen supply and demand produce non-linear plant allocation responses to warming and elevated CO₂. *Proc. Natl Acad. Sci. USA* **16**, 21623–21628 (2019).

20. Colmer, T. D. Long-distance transport of gases in plants: a perspective on internal aeration and radial oxygen loss from roots. *Plant Cell Environ.* **26**, 17–36 (2003).
21. Armstrong, W. in *Advances in Botanical Research* Vol. 7 (ed. Woolhouse, H. W.) 225–332 (Academic Press, 1980).
22. Harriss, R. C. & Matson, P. A. *Biogenic Trace Gases: Measuring Emissions from Soil and Water* (Wiley & Sons, 2009).
23. Bezbaruah, A. N. & Zhang, T. C. Quantification of oxygen release by bulrush (*Scirpus validus*) roots in a constructed treatment wetland. *Biotechnol. Bioeng.* **89**, 308–318 (2005).
24. Schmidt, M. W. I. et al. Persistence of soil organic matter as an ecosystem property. *Nature* **478**, 49–56 (2011).
25. Lehmann, J. & Kleber, M. The contentious nature of soil organic matter. *Nature* **528**, 60–68 (2015).
26. Gunina, A. & Kuzyakov, Y. From energy to (soil organic) matter. *Glob. Change Biol.* **28**, 2169–2182 (2022).
27. Boye, K. et al. Thermodynamically controlled preservation of organic carbon in floodplains. *Nat. Geosci.* **10**, 415–419 (2017).
28. Kirwan, M. L. & Megonigal, J. P. Tidal wetland stability in the face of human impacts and sea-level rise. *Nature* **504**, 53–60 (2013).
29. Smith, A. J., Noyce, G. L., Megonigal, J. P., Guntenspergen, G. R. & Kirwan, M. L. Temperature optimum for marsh resilience and carbon accumulation revealed in a whole ecosystem warming experiment. *Glob. Change Biol.* **28**, 3236–3245 (2022).
30. Cherry, J. A., McKee, K. L. & Grace, J. B. Elevated CO₂ enhances biological contributions to elevation change in coastal wetlands by offsetting stressors associated with sea-level rise. *J. Ecol.* **97**, 67–77 (2009).
31. Pastore, M. A., Megonigal, J. P. & Langley, J. A. Elevated CO₂ and nitrogen addition accelerate net carbon gain in a brackish marsh. *Biogeochemistry* **133**, 73–87 (2017).
32. Noyce, G. L. & Megonigal, J. P. Biogeochemical and plant trait mechanisms drive enhanced methane emissions in response to whole-ecosystem warming. *Biogeosciences* **18**, 2449–2463 (2021).
33. van Bodegom, P. M. & Stams, A. J. M. Effects of alternative electron acceptors and temperature on methanogenesis in rice paddy soils. *Chemosphere* **39**, 167–182 (1999).
34. Liu, L. et al. Methane emissions from estuarine coastal wetlands: implications for global change effect. *Soil Sci. Soc. Am. J.* **83**, 1368–1377 (2019).
35. Yvon-Durocher, G. et al. Methane fluxes show consistent temperature dependence across microbial to ecosystem scales. *Nature* **507**, 488–491 (2014).
36. Dijkstra, F. A. et al. Effects of elevated carbon dioxide and increased temperature on methane and nitrous oxide fluxes: evidence from field experiments. *Front. Ecol. Environ.* **10**, 520–527 (2012).
37. Hutchin, P. R., Press, M. C., Lee, J. A. & Ashenden, T. W. Elevated concentrations of CO₂ may double methane emissions from mires. *Glob. Change Biol.* **1**, 125–128 (1995).
38. Dacey, J. W. H., Drake, B. G. & Klug, M. J. Stimulation of methane emission by carbon dioxide enrichment of marsh vegetation. *Nature* **370**, 47–49 (1994).
39. Ziska, L. H. et al. Long-term growth at elevated carbon dioxide stimulates methane emission in tropical paddy rice. *Glob. Change Biol.* **4**, 657–665 (1998).
40. Bhattacharyya, P. et al. Impact of elevated CO₂ and temperature on soil C and N dynamics in relation to CH₄ and N₂O emissions from tropical flooded rice (*Oryza sativa* L.). *Sci. Total Environ.* **461–462**, 601–611 (2013).
41. Tokida, T. et al. Methane and soil CO₂ production from current-season photosynthates in a rice paddy exposed to elevated CO₂ concentration and soil temperature. *Glob. Change Biol.* **17**, 3327–3337 (2011).
42. Mueller, P. et al. Plants determine methane response to sea level rise. *Nat. Commun.* <https://doi.org/10.1038/s41467-020-18763-4> (2020).
43. Laanbroek, H. J. Methane emission from natural wetlands: interplay between emergent macrophytes and soil microbial processes. A mini-review. *Ann. Bot.* **105**, 141–153 (2010).
44. van der Nat, F.-J. W. A. & Middelburg, J. J. Seasonal variation in methane oxidation by the rhizosphere of *Phragmites australis* and *Scirpus lacustris*. *Aquat. Bot.* **61**, 95–110 (1998).
45. Jordan, T. E. & Whigham, D. F. The importance of standing dead shoots of the narrow leaved cattail, *Typha angustifolia* L. *Aquat. Bot.* **29**, 319–328 (1988).
46. Marsh, A. S., Rasse, D. P., Drake, B. G. & Patrick Megonigal, J. Effect of elevated CO₂ on carbon pools and fluxes in a brackish marsh. *Estuaries* **28**, 694–704 (2005).
47. Drake, B. G. Rising sea level, temperature, and precipitation impact plant and ecosystem responses to elevated CO₂ on a Chesapeake Bay wetland: review of a 28-year study. *Glob. Change Biol.* **20**, 3329–3343 (2014).
48. Erickson, J. E., Megonigal, J. P., Peresta, G. & Drake, B. G. Salinity and sea level mediate elevated CO₂ effects on C3–C4 plant interactions and tissue nitrogen in a Chesapeake Bay tidal wetland. *Glob. Change Biol.* **13**, 202–215 (2006).
49. Frohling, S., Roulet, N. & Fuglestedt, J. How northern peatlands influence the Earth's radiative budget: sustained methane emission versus sustained carbon sequestration. *J. Geophys. Res. Biogeosci.* **111**, G01008 (2006).
50. Ratliff, K. M., Braswell, A. E. & Marani, M. Spatial response of coastal marshes to increased atmospheric CO₂. *Proc. Natl Acad. Sci. USA* **112**, 15580–15584 (2015).
51. Xu, X. & Trugman, A. T. Trait-based modeling of terrestrial ecosystems: advances and challenges under global change. *Curr. Clim. Change Rep.* **7**, 1–13 (2021).
52. Zakharova, L., Meyer, K. M. & Seifan, M. Trait-based modelling in ecology: a review of two decades of research. *Ecol. Model.* **407**, 108703 (2019).
53. Myers-Smith, I. H., Thomas, H. J. D. & Bjorkman, A. D. Plant traits inform predictions of tundra responses to global change. *New Phytol.* **221**, 1742–1748 (2019).
54. Ward, N. D. et al. Representing the function and sensitivity of coastal interfaces in Earth system models. *Nat. Commun.* **11**, 2458 (2020).
55. Moor, H. et al. Towards a trait-based ecology of wetland vegetation. *J. Ecol.* **105**, 1623–1635 (2017).

Publisher's note Springer Nature remains neutral with regard to jurisdictional claims in published maps and institutional affiliations.

Springer Nature or its licensor (e.g. a society or other partner) holds exclusive rights to this article under a publishing agreement with the author(s) or other rightsholder(s); author self-archiving of the accepted manuscript version of this article is solely governed by the terms of such publishing agreement and applicable law.

© Smithsonian Institution, Alexander J. Smith, and Matthew L. Kirwan, under exclusive licence to Springer Nature Limited 2023

Methods

Site description and experimental design

This work was conducted using the Salt Marsh Accretion Response to Temperature Experiment¹⁹ in the Smithsonian's Global Change Research Wetland, a brackish high marsh on the western shore of the Chesapeake Bay, USA (38° 55' N, 76° 33' W). The full experiment consists of 30 plots set up across six warming transects; each plot is 2 × 2 m in area and surrounded by a 0.2 m buffer to mitigate edge effects. Three transects are in a high-elevation area dominated by *Spartina patens* and *Distichlis spicata*, flooded on 10–20% of high tides, and three are in a low-elevation area dominated by *Schoenoplectus americanus*, an herbaceous species that is known to respond rapidly to global change⁵⁶, and flooded on 30–60% of high tides. The *S. americanus* site has an additional eCO₂ treatment.

For this analysis, we used the full subset of 12 plots from the *S. americanus* site that comprise a complete factorial design with two temperature levels (ambient and +5.1 °C of warming) and two CO₂ levels (ambient and +350 ppm). Each treatment combination is replicated three times.

In the warmed plots, above-ground plant-surface temperature is elevated with infrared heaters and soil temperature is elevated with vertical resistance cables¹⁹. Temperature differentials are maintained by integrated microprocessor-based feedback control^{19,57}. Elevated CO₂ plots are surrounded with 2-m-diameter open-top chambers⁹, and CO₂ concentrations are independently controlled in each chamber¹⁹. Warming was initiated in June 2016 and runs year-round. Elevated CO₂ was initiated in April 2017 and is applied during daylight hours throughout the growing season (11 April–30 November 2017; 26 April–6 December 2018; 23 April–18 November 2019; 14 April–11 December 2020). For this analysis, we used the first four years with both warming and eCO₂ treatments.

Vegetation data

Root productivity was assessed using year-long root ingrowth cores, as described previously¹⁹, with three replicate cores per plot. Roots and rhizomes were hand-picked from each core, separated into functional groups, oven-dried at 60 °C, then weighed. Only fine-root biomass was used for further analysis because the high variability introduced by the presence or absence of rhizomes, which the ingrowth cores do not adequately sample, makes it difficult to detect treatment effects on below-ground processes. Outlier data points, typically due to broken cores, were removed using the Grubbs test (1.4% of data), then the remaining replicate cores were averaged to give a per-plot value before statistical tests. Stem productivity was calculated by allometry at peak biomass the first week of August each year¹⁹. Within each 2 m × 2 m treatment plot we censused 30 cm × 30 cm permanent subplots (ambient CO₂; $n = 6$; eCO₂; $n = 5$) for the number, height and width of living stems. Biomass was calculated from the census data using allometric equations⁵⁸, then subplots were averaged per plot before statistical tests.

Redox data

An automated redox system⁵⁹ was installed in all six of the +5.1 °C plots (three each at ambient and elevated CO₂) in March 2020 and has operated continuously ever since. An extension to the system was installed in all six of the ambient-temperature plots in 2022. Each plot has six redox probes with platinum bands at 5 and 20 cm below the soil surface and two Ag|AgCl (saturated KCl) reference electrodes (Paleo Terra). The probes are connected to an AM16/32B multiplexer (Campbell Scientific) and a CR1000 datalogger (Campbell Scientific,) powered by a solar-charged battery that is not grounded externally. Redox potential was measured every 30 min, during which the power to soil heating was paused to minimize interference. Data were corrected to the standard hydrogen electrode before analysis by adding 202 to the raw millivolt reading. Replicate measurements within a plot were averaged for each

time point ($n = 6$) and then averaged again ($n = 48$) for a daily mean per plot before statistical tests.

NOSC data

Fourier-transform ion cyclotron resonance analysis was conducted at the Environmental Molecular Sciences Laboratory, a Department of Energy Office of Science user facility sponsored by the Office of Biological and Environmental Research. Duplicate 10 ml porewater samples were acidified and passed through a solid-phase extraction clean-up procedure to remove salts using Bond-Elut SPE cartridges (Agilent). The cartridges were rinsed with 200 ml of 10 mM HCl due to the high salt content. Samples were then infused into the 21 T Fourier-transform ion cyclotron resonance mass spectrometer by an automated direct injection system at a flow rate of 4 $\mu\text{m} \text{min}^{-1}$. Samples were co-added for 500 small-angle neutron scattering, 220–900 Da. Data were peak-picked using a S/N of 3 and the in-house software NOMSI. Data were further calibrated, aligned and assigned to formulas using the in-house software Formularity. To conservatively estimate treatment effects, only peaks that were detected in both replicates were included in further analysis. The NOSC values of all identified compounds were then averaged to give a per-plot estimate.

Surface elevation table data

Soil surface elevations were tracked using surface elevation tables (SETs)^{60,61}. In June 2016, SET benchmarks were installed in each plot outside of the experimental plots by driving a series of stainless-steel rods through the entire soil profile to refusal and then permanently anchoring them⁶². Elevation measurements were collected from approximately 70 fibreglass 3 mm circular rods or 'pins' that gauge the distance from a parallel bar attached to the anchored benchmark to the ground and recorded to the nearest millimetre. This resulted in high-precision measurements of soil surface elevations relative to the base of the benchmark. Measurements reported in this study were taken every June, August and January since January 2017, except for a period from March 2019 to February 2020 when measurements were taken every two months. Spatial dependence between pins was calculated using a gamma autocorrelation metric to determine that measurements became independent approximately 27 mm (or approximately 6 pins) from one another. To determine long-term trends, marsh surface elevation was regressed against time for each SET pin, resulting in approximately 60 estimates of linear trends for each plot. Per-pin linear regressions across replicate plots (~180 linear regressions per treatment) were then averaged to estimate the average long-term change in elevation at the treatment level.

Methane data

Methane emissions and porewater were measured as described in ref. ³². The CH₄ fluxes were measured monthly in all four years, using static chambers and an Ultraportable Greenhouse Gas Analyzer (Los Gatos Research). Fluxes were calculated as the linear rate of change of CH₄ concentration in the chamber headspace over 5 min. Fluxes were averaged across June, July and August to give one summer flux estimate per plot to use for statistical tests.

Porewater was collected in May, July and September of each year from duplicate stainless-steel sippers permanently installed at 10, 20, 40, 80 and 120 cm below the peat surface. Methane was extracted from the porewater and analysed on a Shimadzu GC-FID. Porewater data were averaged across all depths ($n = 5$) for each sampling period and then averaged per plot ($n = 3$) before statistical tests.

Radiative forcing calculations

Net radiative forcing was calculated as the sum of carbon uptake or loss as estimated by soil carbon accumulation rates and annual CH₄ emissions. Carbon accumulation rates were calculated as the product of the change in soil elevation in each plot from January 2017 to August

2020 and the average carbon density of all plots (104.8 kgC m^{-3}) (ref. ²⁹). Monthly CH_4 flux measurements were scaled to annual estimates by regressing $\log \text{CH}_4$ emissions against daily mean soil temperature and day of year as a proxy for phenological status³². Including day of year accounts for the observation that the relationship between CH_4 emissions and temperature is hysteretic, with CH_4 emissions being higher at a given temperature in the fall than in the spring. Individual linear regressions were calculated for each plot and year, and the coefficients were used to interpolate between measurement dates. Model summary statistics are reported in Supplementary Table 1. The radiative forcing effects of warming and eCO_2 treatments were calculated using a sustained-flux global warming potential for CH_4 of 45 relative to CO_2 over a 100 yr period⁶³.

Statistical analysis

All statistics were conducted in R, version 4.0.2. Methane data were log-transformed to correct for non-normality before analysis. For biomass, redox, NO₃⁻, methane and radiative forcing, statistics were conducted on treatment means ($n = 3$) using data that had previously been summarized per plot as described in the preceding. The effects of warming and eCO_2 were determined using two-way analysis of variance followed by Tukey's honestly significant difference as post hoc tests. For redox data, the two treatments were compared using a t test.

Data availability

The data that support the findings of this study are available from the corresponding authors upon request and in the Smithsonian Institution figshare repository (<https://smithsonian.figshare.com>) under <https://doi.org/10.25573/serc.21263328>.

References

- Langley, J. A. & Megonigal, J. P. Ecosystem response to elevated CO_2 levels limited by nitrogen-induced plant species shift. *Nature* **466**, 96–99 (2010).
- Rich, R. L. et al. Design and performance of combined infrared canopy and belowground warming in the B4WarmED (Boreal Forest Warming at an Ecotone in Danger) experiment. *Glob. Change Biol.* **21**, 2334–2348 (2015).
- Lu, M. et al. Allometry data and equations for coastal marsh plants. *Ecology* **97**, 3554–3554 (2016).
- Rabenhorst, M. C., Hively, W. D. & James, B. R. Measurements of soil redox potential. *Soil Sci. Soc. Am. J.* **73**, 668–674 (2009).
- Cahoon, D. R. et al. High-precision measurements of wetland sediment elevation: I. Recent improvements to the sedimentation–erosion table. *J. Sediment. Res.* **72**, 730–733 (2002).
- Cahoon, D. R. et al. High-precision measurements of wetland sediment elevation: II. The rod surface elevation table. *J. Sediment. Res.* **72**, 734–739 (2002).
- Lynch, J. C., Hensel, P. & Cahoon, D. R. *The Surface Elevation Table and Marker Horizon Technique: A Protocol for Monitoring Wetland*

Elevation Dynamics Natural Resource Report NPS/NCBN/NRR—2015/1078 (USGS, 2015); <http://pubs.er.usgs.gov/publication/70160049>

- Neubauer, S. C. & Megonigal, J. P. Moving beyond global warming potentials to quantify the climatic role of ecosystems. *Ecosystems* **18**, 1000–1013 (2015).

Acknowledgements

We thank G. Peresta for maintaining the field experiment and S. Kent, T. Messerschmidt, E. Herbert and D. Walters for assisting with field measurements. Funding for this project was provided by the US Department of Energy, Office of Science, Office of Biological and Environmental Research, Environmental System Science programme under award numbers DE-SC0014413 to J.P.M., M.L.K. and R.L.R. and DE-SC0019110 and DE-SC0021112 to J.P.M., G.L.N., M.L.K. and R.L.R.; the National Science Foundation Long-Term Research in Environmental Biology Program under award numbers DEB-0950080, DEB-1457100 and DEB-1557009 to J.P.M. and DEB-2051343 to J.P.M. and G.L.N.; and the Smithsonian Institution to J.P.M., G.L.N. and R.L.R. A portion of the research was performed using EMSL, a DOE Office of Science user facility sponsored by the Office of Biological and Environmental Research, under user project 50205 to G.L.N. and J.P.M.

Author contributions

J.P.M., R.L.R., G.L.N. and M.L.K. designed the original experiment, R.L.R. designed the feedback-controlled heating system and G.L.N. and R.L.R. designed the redox measurement system. G.L.N. collected and analysed all vegetation and biogeochemical data and wrote the initial manuscript. A.J.S. provided SET data and analysis. All authors contributed to interpreting results and editing the manuscript.

Competing interests

The authors declare no competing interests.

Additional information

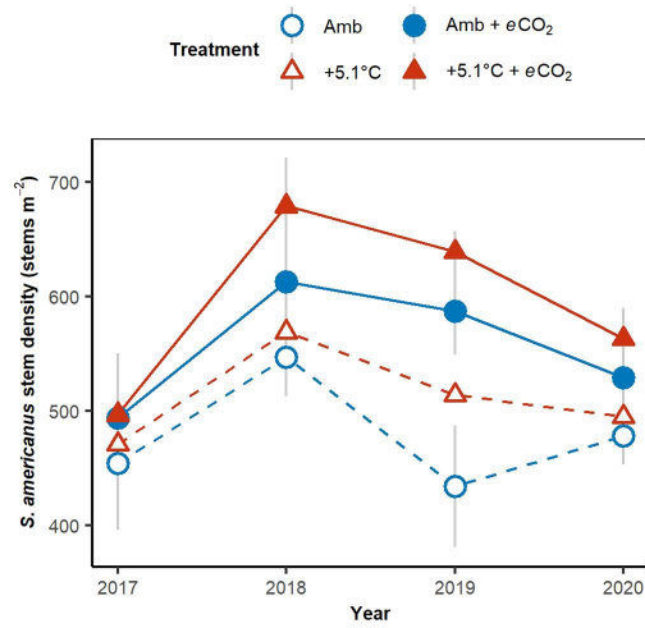
Extended data is available for this paper at <https://doi.org/10.1038/s41561-022-01070-6>.

Supplementary information The online version contains supplementary material available at <https://doi.org/10.1038/s41561-022-01070-6>.

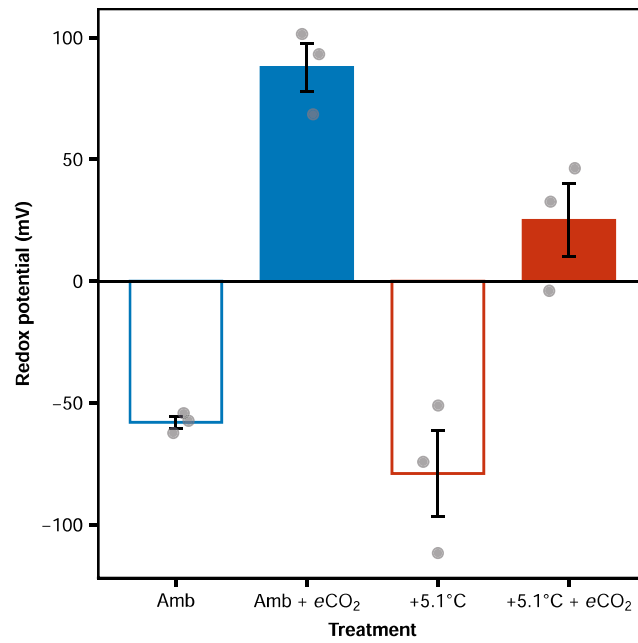
Correspondence and requests for materials should be addressed to Genevieve L. Noyce or J. Patrick Megonigal.

Peer review information *Nature Geoscience* thanks Jorge Villa and the other, anonymous, reviewer(s) for their contribution to the peer review of this work. Primary Handling Editor: Xujia Jiang, in collaboration with the *Nature Geoscience* team.

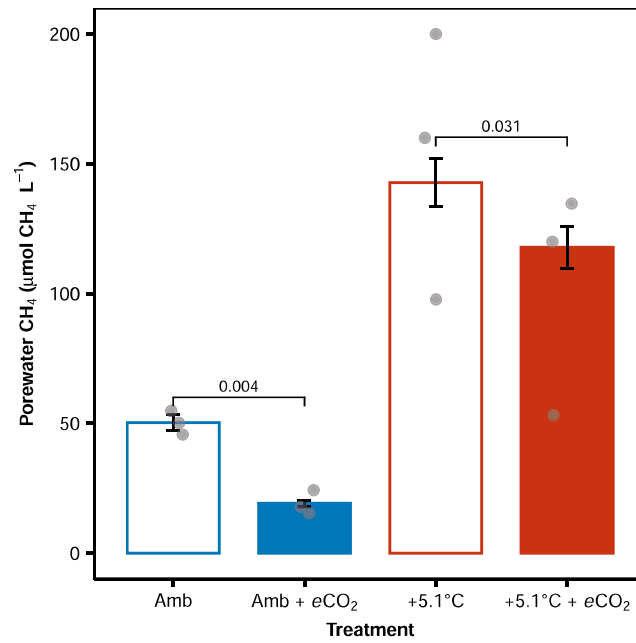
Reprints and permissions information is available at www.nature.com/reprints.



Extended Data Fig. 1 | Annual *Schoenoplectus americanus* stem density in all treatments from 2017 to 2020. Points are means of triplicate plots. Error bars are standard error across treatment replicates ($n = 3$). Temperature treatments are ambient (Amb) or +5.1 °C above ambient (+5.1 °C) either alone or crossed with elevated CO₂ (+eCO₂).



Extended Data Fig. 2 | Mean redox potential measured at 5 cm depth in spring 2022 (Apr through Jun). Error bars are standard error across treatment replicates ($n = 3$). Temperature treatments are ambient (Amb) or +5.1 °C above ambient (+5.1 °C) either alone or crossed with elevated CO₂ (+eCO₂).



Extended Data Fig. 3 | Mean porewater CH₄ (10–120 cm) from all treatments. Samples were collected in May, Jun, and Sep. Brackets above the paired bars show the P values for the differences between treatments based on Tukey's HSD test. Elevated CO₂ significantly reduced porewater CH₄ in both ambient and warmed

treatments. Error bars are standard error across treatment replicates ($n = 3$). Temperature treatments are ambient (Amb) or +5.1°C above ambient (+5.1°C) either alone or crossed with elevated CO₂ (+eCO₂).